Available online at www.sciencedirect.com
ScienceDirect
Journal of Photochemistry and Photobiology B: Biology 89 (2007) 125–130
Journal of Photochemistry and Photobiology B:Biology
www.elsevier.com/locate/jphotobiol

The effect of the association of NIR laser therapy BMPs, and guided bone regeneration on tibial fractures treated with wire osteosynthesis: Raman spectroscopy study

C.B. Lopes [a], M.T.T. Pacheco [b], L. Silveira Jr. [b], J. Duarte [b], M.C.T. Cangussú [c], A.L.B. Pinheiro [d,e,*]

[a] *Laser Center, IP&D, FCS, UNIVAP, S.J. Campos, SP 12244-000, Brazil*
[b] *Laboratory of Biomolecular Spectroscopy, IP&D, UNIVAP, S.J. Campos, SP 12244-000, Brazil*
[c] *School of Dentistry, Federal University of Bahia, Salvador 40110-150, Brazil*
[d] *Laser Center, IP&D, UNIVAP, S.J. Campos, SP 12244-000, Brazil*
[e] *Laser Center, School of Dentistry, Federal University of Bahia, Av. Araújo Pinho, 62, Canela, Salvador 40110-150, BA, Brazil*

Received 16 May 2007; received in revised form 14 September 2007; accepted 27 September 2007
Available online 1 October 2007

Abstract

Bone fractures are lesions of different etiology; may be associated or not to bone losses; and have different options for treatment, such as the use of biomaterials, guided bone regeneration, techniques considered effective on improving bone repair. Laser therapy has also been shown to improve bone healing on several models. The association of these three techniques has been well documented by our group using different models. This study aimed to assess, through Raman spectroscopy, the incorporation of calcium hydroxyapatite (CHA $\sim 958\ cm^{-1}$) on the repair of complete tibial fractures in rabbits treated with wire osteosynthesis (WO); treated or not with laser therapy; and associated or not with the use of BMPs and/or Guided Bone Regeneration. Complete tibial fractures were created in 12 animals that were divided into four groups: WO; WO + BMPs; WO + laser therapy; and WO + BMPs + laser therapy. Irradiation started immediately after surgery; was repeated at every other day during 2 weeks; and was carried out with λ 790 nm laser light (4 J/cm^2 per point, 40 mW, $\varphi \sim 0.5\ cm^2$, 16 J per session). Animal death occurred after 30 days. Raman spectroscopy was performed at both the surface and the depth of the fracture site. Statistical analysis showed significant difference on the concentrations of CHA between surface and depth. The analysis in each of the areas showed at the depth of the fracture significant differences between all treatment groups ($p < 0.0001$). Significant differences were also seen between WO + BMPs + laser therapy and WO ($p < 0.001$) and WO + laser therapy ($p < 0.001$). At the surface, significant difference was seen only between the treatment groups and the non-fractured subjects ($p = 0.0001$). However, no significant difference was seen between the treatment groups ($p = 0.14$). It is concluded that the use of NIR laser therapy associated to BMPs and GBR was effective in improving bone healing on the fractured bones as a result of the increasing deposition of CHA measured by Raman spectroscopy.

Keywords: Bone healing; Internal rigid fixation; Laser therapy; LLLT

1. Introduction

The healing of a fracture is an extremely interesting process in the human body. In optimal conditions, injured bone can be reconstituted without a scar almost identically to its original shape. Bone healing has been under extensive investigation for many years.

* Corresponding author. Address: Laser Center, School of Dentistry, Federal University of Bahia, Av. Araújo Pinho, 62, Canela, Salvador 40110-150, BA, Brazil. Tel.: +55 71 3336 4343x246.
E-mail address: albp@ufba.br (A.L.B. Pinheiro).

1011-1344/$ - see front matter © 2007 Elsevier B.V. All rights reserved.
doi:10.1016/j.jphotobiol.2007.09.011

The treatment of fractures consists of the reduction and fixation of dislocated segments [1]. Wires are used alone or, more commonly, in combination with other orthopedic fixation devices. Wires are of various diameters; can be braided; are frequently used to reattach osteotomized bone fragments; are used to suture bone and soft tissue; and they can break. However, breakage of wires is usually of little significance.

Since the late 1950s, open reduction and internal fixation of fractures have been used to restore bone anatomy and enable early mobilization. These procedures also overcame the limitations encountered when fractures are treated with skeletal traction or cast immobilization. The use of internal fixation in the treatment of fractures shall provide sufficient stability for fracture healing without excessive rigidity. The choice of the method of internal fixation depends on the type of fracture; on the condition of the soft tissues and bone; on the size and position of the bone fragments; and the size of the bony defect.

The main goal of internal fixation is the achievement of prompt and, if possible, full function of the injured bone, with rapid rehabilitation of the patient. The majority of internal fixation devices are currently made of stainless steel. Occasionally, less strong, but biologically superior and more elastic, titanium implants are favored. Numerous devices are available for internal fixation. These devices can be roughly divided into a few major categories: wires; pins and screws; plates; and intramedullary nails or rods. Staples and clamps are also used occasionally for osteotomy or fracture fixation.

Stainless steel wire is the traditional material used for fracture fixation because it is a biologically inert material; rigidity; provides precise repositioning of the bone fragments; it is easy to use; and has a reasonable cost [2]. The treatment of fractures has significantly advanced over the years due to improved understanding of the biomechanical principles; advances in biomaterials; and instrumentation [3].

There are fractures in which handling is further complicated due to the loss of bone. These losses may be related to several etiologies and require further efforts from the body to fully recover. Although grafts have been used to minimize the problems associated to bone losses, considerable limitations associated with autografts and allografts have prompted increased interest in alternative bone graft substitutes [4,5].

The development and use of bone graft substitutes is a burgeoning field, and review of all available products and indications is beyond the scope of this paper. The main types of commercially available bone graft substitutes are demineralized allograft bone matrix; ceramics and ceramic composites; composite graft of collagen and mineral; coralline hydroxyapatite; calcium phosphate cement; bioactive glass; and calcium sulfate [4–6].

The treatment of bone defects using biomaterials has been extensively studied elsewhere [4–7]. Since the pioneer work by Urist that demonstrated heterotrophic formation of bone induced by devitalized demineralized bone matrix (DBM), a new possibility of treating bone defects has surfaced [7,8].

The healing of various types of bone defect with complete bone fill has been reported following the application of the Guided Bone Regeneration – GBR technique [9]. GBR is a technique used to prevent the migration of soft tissues, which has more pronounced proliferative activity, into the bone defect. GBR promotes bone formation by the use of a mechanical barrier such as membranes and these may be reabsorbable or non-reabsorbable and may also be associated or not to bone substitutes. The GBR is widely used for treating periodontal defects and other bone defects [7].

Many techniques are used to improve the bone healing, recently, laser therapy has been used for improving bone healing in several conditions, such as in dental implants [10] and autologous bone graft [5], and several types of bone defects [4–7]. Several studies have demonstrated that NIR laser therapy is the most suitable method for bone repair due to its higher penetration depth in the bone tissue when compared to visible laser light [7]. Although the use of laser therapy on the bone healing has been growing steadily and several studies have demonstrated positive results on the healing of bone tissue, there are a few reports on the association of laser therapy and biomaterials [4,7].

The Raman spectroscopy is an optical tool, which could permit less invasive and nondestructive analysis of biological samples, allowing one to get precise information on biochemical composition [12,13]. It has been considered effective to assess tissues at the molecular level, and has been used on several non-invasive diagnostic applications of biological samples such as cancers [11]; human coronary arteries [12,13]; blood analysis [14]; implants [15,16]; cell culture [17]; bone diseased [18]; bone healing [10,17,19]; to evaluate the microstructure of human cortical bone (osteon) [19] and biomaterials [20]. Raman spectroscopy has been accepted by many as a viable tool for the study of bone mineralization. The infrared spectroscopy was preferred over Raman spectroscopy, principally due to the interference of Raman spectra with fluorescence from biological specimens [17].

In a recent study [10], Raman spectroscopy was used to investigate the effects of laser therapy on the healing of dental implant of rabbits by monitoring the level of Calcium Hydroxyapatite in 15, 30 and 45 days after surgery. It was concluded that the use of laser therapy was effective in improving bone healing as a result of the increasing deposition of CHA, this being measured by Raman spectroscopy.

The aim of this study was to evaluate, through the analysis of Raman spectra intensity, the incorporation of calcium hydroxyapatite (CHA; 958 cm^{-1}; phosphate ν_1) on the repair of complete tibial fracture in rabbits treated by wire osteosynthesis associated or not to the use of laser therapy (λ 790 nm) and/or not to the use of BMPs and Guided Bone Regeneration by measuring the alteration

of the CHA band and relating this alteration to the healing promoted by the photobiomodulation.

2. Materials and methods

This study was approved by the Animal Ethics Committee of the Universidade do Vale do Paraíba. Twelve healthy adult male New Zealand rabbits (average weight 2 kg) were kept under natural conditions of light, humidity, and temperature at the Animal House of the Instituto de Pesquisa e Desenvolvimento da Universidade do Vale do Paraíba during the experimental period. The animals were fed with standard laboratory pelted diet and had water *ad libidum*. The animals were kept in individual metallic gages; kept at day/night light cycle and controlled temperature during the experimental period.

Under general anesthesia (0.2% Acepran®, 1 mg/kg, Univet S.A, São Paulo, SP, Brazil, Butorfanol® 0.02 ml/kg, Fort Dodge Ltda, Campinas, SP, Brazil; and Zoletil® 50 mg, 15 mg/kg, VIRBAC S.A, Carro Cedex, France), the animals had the right leg shaved and a 4-cm long incision was performed at the right tibia with a n° 15 scalpel blade. Skin and subcutaneous tissues were dissected down to the periosteum, which was gently sectioned exposing the bone. One tibial complete bone fracture was surgically produced (low speed drill, 1200 rpm, under refrigeration) in each animal. The random distribution of the animals can be seen on Table 1.

All groups had open fracture reduction and fixation with wire osteosynthesis (Stainless steel 0.30 mm, Morelli®). On groups G2 and G4, the defect was filled with lyophilized organic bovine bone (Gen-ox-org®, Baumer S/A, Mogi Mirim, SP, Brazil), collagen (Gen-col®, Baumer S/A, Mogi Mirim, SP, Brazil), bone morphogenetic proteins (Gen-pro®, Baumer S/A, Mogi Mirim, SP, Brazil) and covered with decalcified cortical osseous membrane (Gen-derm®, Baumer S/A, Mogi Mirim, SP, Brazil). On groups G3 and G4, laser therapy (λ 790 nm, 40 mW, $\varphi \sim 0.5\ cm^2$) was transcutaneously applied in 4 points around the defects at 48-h intervals (4 J/cm^2, per point) being the first session carried out immediately after surgery and repeated at every 48 h for 15 days (16 J/cm^2 per session) and a total treatment dose of 112 J/cm^2. To standardize the location of irradiation, four tattoos were made on the skin using Nankin Ink around the fracture immediately after surgery to allow irradiation to be carried out at the same point. Doses used here are based upon previous studies carried out by our group [4].

Table 1
Distribution of each animal on the experimental group

Group	Treatment	Biomaterial + ROG	Laser therapy
I	Wire osteosynthesis	No	No
II	Wire osteosynthesis	Yes	No
III	Wire osteosynthesis	No	Yes
IV	Wire osteosynthesis	Yes	Yes

All wounds were routinely sutured and the animals received a single dose of pentabiotico® (penicillin, streptomycin, 20.000UI, Fort Dodge Ltda, Campinas, SP, Brazil), immediately after surgery. The animals were humanely killed 30 days after the surgery with an overdose of general anesthetics.

The samples were longitudinally cut under refrigeration (Bueler®, Isomet TM1000; Markham, Ontario, Canada) and the specimens were stored in liquid nitrogen to minimize the growth of aerobic bacteria [10,12,13], and because the chemical fixation is not advisable due to fluorescence emissions from the fixative substances [10,12,13].

Prior to Raman study, the samples were longitudinally cut and warmed gradually to room temperature and 100 ml of saline was added to the surface during spectroscopic measurements. For Raman measurements an $\lambda = 830$ nm Ti: Sapphire laser (Spectra Physics, model 3900S, Mountain View, CA, USA) pumped by Argon laser (Spectra Physics, model 2017S, Mountain View, CA, USA) provided near-infrared excitation. A spectrograph (Bruker Optics, model: 250 IS; Billerica, MA, USA) with spectral resolution of about 8 cm^{-1} dispersed the Raman scattered light from the sample and a liquid-nitrogen cooled deep depletion CCD (Princeton Instruments, model LN/CCD-1024-EHR1; Tucson, AZ; USA) detected the Raman spectra. The system was controlled by a microcomputer, which stored and processed the data [10,12,13]. The laser power used at the sample was of 80 mW, spectral acquisition time 100 s. Four points were measured in the transversal cut of the bone healing resulting in four readings of each specimen and 52 total spectra. All spectra were collected at the same day to avoid optical misalignments and changes in laser power. The mean value of the intensity of the peak (958 cm^{-1}, phosphate ν_1) was determined by the average of the peaks in this region. This intensity is related to the concentration of CHA on the bone. The data were analyzed by the MatLab5.1® software (Newark, New Jersey, USA) for calibration and background subtraction of the spectra. For

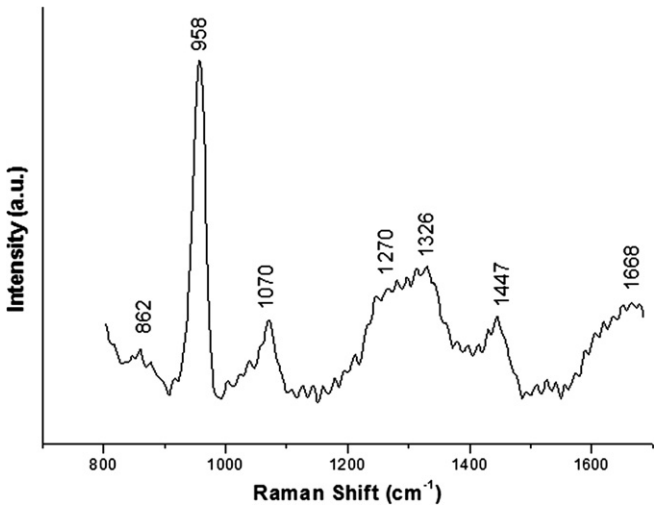

Fig. 1. Characteristic Raman spectrum of CHA (958 cm^{-1}, phosphate ν_1).

calibration, the Raman spectrum of a solvent indene with known peaks was used [10,12,13] due to its intense bands in the region of (800–1800 cm^{-1}) our interest. The indene spectrum was also measured each time the sample was changed to be sure that the laser and collection optics were optimized. To remove the "fluorescence background" from the original spectrum, a fifth order polynomial fitting was found to give better results facilitating the visualization of the peaks of CHA (~958 cm^{-1}) found in the bone (Fig. 1). This routine can also remove any continuum, offset background noise, due to CCD read out and cooling. Statistical analysis was performed using Minitab 12.0® software (Minitab, Belo Horizonte, MG, Brazil).

3. Results

The Raman spectrum of bone shows prominent vibrational bands related to tissue composition. Fig. 1 shows the tissue main Raman bands at 862, 958, 1070, 1270, 1326, 1447 and 1668 cm^{-1}. The 1668 cm^{-1} band and the ones at 1270 and 1326 cm^{-1} are attributed to amide I and amide III stretching modes, the ones at 958 and 1070 cm^{-1} are attributed to phosphate and carbonate hydroxyapatite, respectively. The band at 862 cm^{-1} can be attributed to the vibration bands of C–C and C–C–H stretch of collagen and lipid. The band at 1447 cm^{-1} is attributed to the bending and stretching modes of CH groups of lipids and proteins [20]. Figs. 2 and 3 show differences on the intensity of the Raman band at 1447 cm^{-1} between treated and untreated groups. The peak intensity of the untreated group was higher than on the treated groups.

The value of the mean intensity of each Raman shift of hydroxyapatite (CHA) was obtained from all readings taken in each group on both surface and depth of the fractured area (Figs. 2 and 3). The intensity of the Raman shift

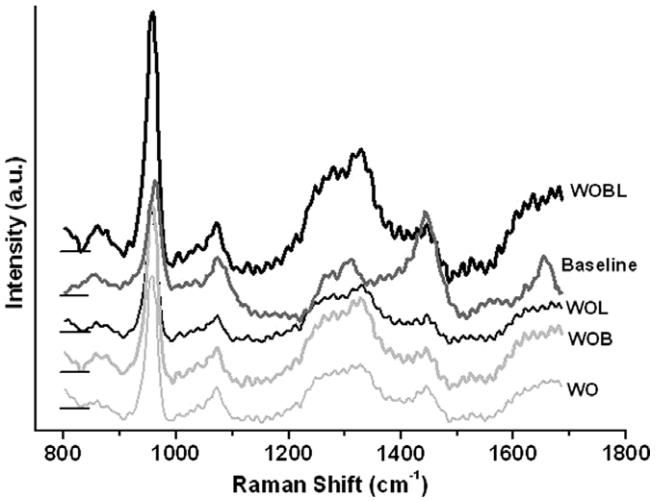

Fig. 3. Mean Raman shift of the concentration of CHA (~958 cm^{-1}) on the depth of tibial fractures treated with wire osteosynthesis.

is directly related to the concentration/incorporation of CHA by the bone. So, higher intensity represents higher concentration of CHA. The results of the mean readings can be seen on Table 2.

Statistical analysis of the readings of both areas (surface/depth) evidenced no significant difference on the concentrations of CHA between the two areas (T-test with Welch correction, $p = 0.29$). The analysis of each area showed significant differences between all treatment groups (Anova, $p < 0.0001$) at the depth of the fracture. Significant differences were also seen between subjects treated with wire osteosynthesis + BMPs + laser therapy and wire osteosynthesis (Turkey–Kramer Test, $p < 0.001$) and wire osteosynthesis + laser therapy (Turkey–Kramer, $p < 0.001$) (Fig. 4). At the surface of the lesion, significant difference was seen between the treatment groups and non-fractured (baseline) subjects (Kruskal–Wallis, $p = 0.0001$). However,

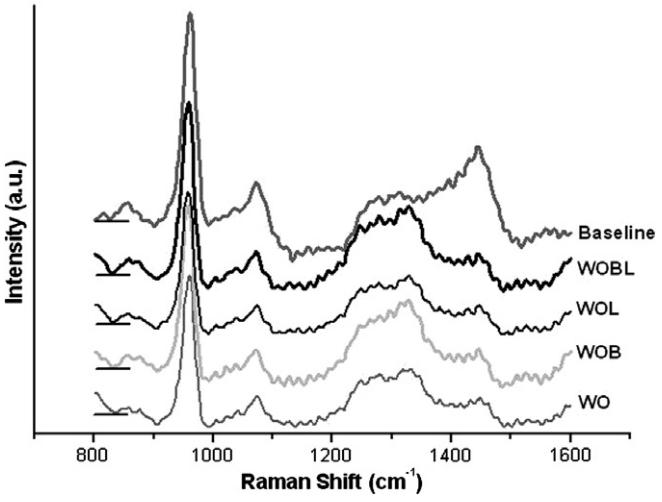

Fig. 2. Mean Raman shift of the surface concentration of CHA (~958 cm^{-1}) on the surface of tibial fractures treated with wire osteosynthesis.

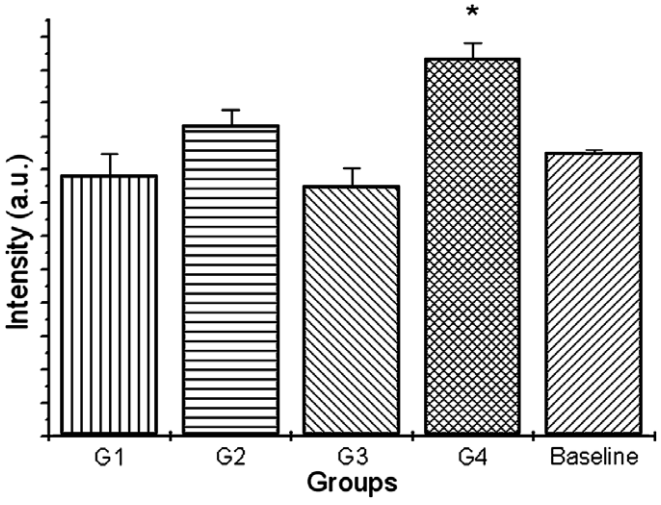

Fig. 4. Averages of intensities of CHA (~958 cm^{-1}) on the depth of tibial fractures treated with wire osteosynthesis. *Significance level 0.05.

Table 2
Mean Raman shift (~958 cm^{-1}) of CHA on the both areas (surface/depth) treated with wire osteosynthesis

	Baseline (non-treated bone)	Group I (wire osteosynthesis)	Group II (wire osteosynthesis + BMP)	Group III (wire osteosynthesis + laser therapy)	Group IV (wire osteosynthesis + BMPs + laser therapy)
Surface	11974 ± 209*	8018 ± 399*	9121 ± 621*	7860 ± 340*	9198 ± 641*
Depth	8520.3 ± 75*	7829 ± 635*	9323 ± 476*	7514 ± 543*	11350 ± 473*

* Standard error of mean.

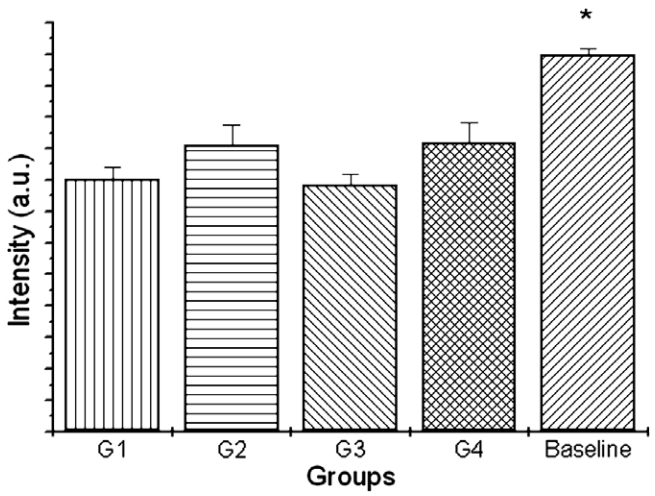

Fig. 5. Averages of intensities of CHA (~958 cm^{-1}) on the surface of tibial fractures treated with wire osteosynthesis. *Significance level 0.05.

no significant difference was seen between the treatment groups (Anova, $p = 0.14$, Fig. 5).

4. Discussion

Laser therapy has been successfully used for improving bone healing in several conditions [4]. The effects of laser therapy on bone are still controversial, as previous reports show different or conflicting results. It is possible that the effect of laser therapy on bone regeneration depends not only on the total dose of irradiation, but also on the irradiation time and the irradiation mode [4]. Many studies indicated that irradiated bone, mostly with IR wavelengths, shows increased osteoblastic proliferation, collagen deposition, and bone neoformation when compared to non-irradiated bone [4]. The irradiation protocol used in this study is similar to those used on previous reports [4–7,10]. Our group has shown, using different models, that the association of bone grafts, BMPs and Guided Tissue Regeneration does improve the healing of bone tissue [4].

Raman spectroscopy can be used to access the molecular constitution of a specific tissue and then classify it according to the differences observed in the spectra [13]. Several studies found elsewhere in the literature have shown successful use of NIRS as a diagnostic tool for healthy, diseased or healing bones [10,15–19].

The present investigation analyzed, by NIRS, the intensity of the shift of the CHA (~958 cm^{-1}) on the sites of complete tibial fractures in rabbits. The fractures were routinely treated by open reduction and internal fixation using wire osteosynthesis. Due to the lack of report of the use of this model in the literature, the complete understanding of these initial findings is difficult. There are several aspects to consider in regards to the technique used. Initially, it is important to consider that the repair of fractured bones is lengthy, when compared to other types of bony defects, and demands stability of the fragments not to develop non-union. In our study, no such case was found.

We have previously found that the levels of CHA on deep areas of healing bone of irradiated and non-irradiated subjects differ significantly from day 30 after treatment [10]. On this study, we were able to detect the differences on the CHA levels of fractured sites when internal fixation was associated to the use of biomaterials, GBR and laser therapy. This is in complete agreement with the reports in the literature [4].

It is important to note that, despite not being statistically significant, the results of the measurements of the levels of CHA at the surface of the fractured site are encouraging as all the treatment showed the same level of CHA deposition. It is also important to consider that the wavelength used has a deeper penetration on the tissue and less surface absorption, This aspect may have, in some way, affected differently the two areas. It is also to be considered that the deep area of the bone has a larger number of cells and these are more effectively affected by laser therapy [4,10].

We found a difference on the intensity of the 1447 cm^{-1} peak between untreated and treated groups. This peak may be related to the lipid's content of the bone. Untreated subjects showed higher peak intensity than the treated ones. This may be a result of the conversion of yellow medulla on red medulla during the healing [21].

It is known that laser therapy has the ability to stimulate cell proliferation, including fibroblasts; this cell has the capacity to secrete collagen. The use of the organic bone graft associated to laser therapy resulted in better repair than that observed when the graft was used alone. Similar observations were reported previously [4,7]. This may represent an improved ability of more mature osteoblasts to secrete CHA on irradiated subjects, whereas in others groups, cell proliferation was still occurring. Deposition of CHA represents bone maturation. The results of this study indicate that laser therapy associated to biomaterial grafts and GBR, increased the concentration of CHA.

Increased amount of CHA in bone is indicative of a more resistant bone [4,5,7,10].

It is concluded that the use of NIR laser therapy associated to BMPs and GBR was effective in improving bone healing on fractured bones as a result of the increasing deposition of CHA measured by Raman spectroscopy.

References

[1] Ö. Erdogan, E. Esen, Y. Ustun, M. Kurkçu, T. Akova, G. Gonlusen, H. Uysal, F. Çevlik, Effects of low-intensity pulsed ultrasound on healing of mandibular fractures: an experimental study in rabbits, J. Oral Maxillofac. Surg. 64 (2006) 180–188.
[2] W.C. Broaddus, K.L. Holloway, C.J. Winters, M.R. Bullock, R.S. Graham, B.E. Mathern, J.D. Ward, H.F. Young, Titanium miniplates or stainless steel wire for cranial fixation: a prospective randomized comparison, J. Neurosurg. 96 (2002) 244–247.
[3] J.R. Fernández, M. Gallas, M. Burguera, J.M. Viãno, A three-dimensional numerical simulation of mandible fracture reduction with screwed miniplates, J. Biomech. 36 (2003) 329–337.
[4] A.L.B. Pinheiro, M.E. Gerbi, Photoengineering of bone repair processes, Photomed. Laser Surg. 24 (2006) 169–178.
[5] J.B. Weber, A.L.B. Pinheiro, M.G. Oliveira, M.G.O. Oliveira, L.M.P. Ramalho, Laser therapy improves healing of bone defects submitted to autologous bone graft, Photomed. Laser Surg. 24 (2006) 38–44.
[6] A.L.B. Pinheiro, F.A. Limeira Júnior, M.E.M.M. Gerbi, L.M.P. Ramalho, C. Marzola, E.A.C. Ponzi, Effect of low level laser therapy on the repair of bone defects grafted with inorganic bovine bone, Braz. Dent. J. 14 (2003) 177–181.
[7] M.E.M.M. Gerbi, A.L.B. Pinheiro, C. Marzola, F.A. Limeira Júnior, L.M.P. Ramalho, E.A.C. Ponzi, A.O. Soares, L.C.B. Carvalho, H.C.A.V. Lima, T.O. Gonçalves, Assessment of bone repair associated with the use of organic bovine bone and membrane irradiated at 830-nm, Photomed. Laser Surg. 23 (2005) 382–388.
[8] R. Dimitriou, P.V. Giannoudis, Discovery and development of BMPs, Int. J. Care Inj. 365 (2005) 528–533.
[9] N. Donos, L. Kostopoulos, T. Karring, Augmentation of the mandible with GTR and onlay cortical bone grafting. An experimental study in the rat, Clin. Oral Implants Res. 13 (2002) 175–184.
[10] C.B. Lopes, A.L.B. Pinheiro, S. Sathaiah, J. Duarte, M.C. Martins, Infrared laser light reduces loading time of dental implants: a Raman spectroscopy study, Photomed. Laser Surg. 23 (2005) 27–31.
[11] A.P. Oliveira, R.A. Bitar, L. Silveira, R.A. Zangaro, A.A. Martin, Near-infrared Raman spectroscopy for oral carcinoma diagnosis, Photomed. Laser Surg. 24 (2006) 348–353.
[12] L. Silveira-Júnior, S. Sathaiah, R.A. Zângaro, M.T.T. Pacheco, M.C. Chavantes, C.A. Pasqualucci, Near infrared Raman spectroscopy of human coronary arteries: histopathological classification based on Mahalanobis distance, J. Clin. Laser Med. Surg. 21 (2003) 203–208.
[13] G.V. Nogueira, L. Silveira Júnior, A.A. Martin, R.A. Zângaro, M.T.T. Pacheco, M.C. Chavantes, C.A. Pasqualucci, Raman spectroscopy study of atherosclerosis in human carotid artery, J. Biomed. Opt. 10 (2005) 031117-1–031117-7.
[14] S. Pilotto, A.B. Villaverde, M.T.T. Pacheco, L. Silveira, R.A. Zângaro, Analysis of near-infrared Raman spectroscopy as a new technique for transcutaneous non-invasive diagnosis of blood components, Laser Med. Sci. 16 (2001) 2–9.
[15] H. Yuan, Z. Yang, Y. Li, X. Zhang, J.D. Bruijn, K. Groot, Osteoinduction by calcium phosphate biomaterials, J. Mater. Sci Mater. Med. 9 (1998) 723–726.
[16] K. Ohsaki, A. Shibata, K. II, Q. Ye, Y.H. Tran, S. Yamashita, Long-term microstructural analyses of hydroxyapatite implanted in rats using laser-Raman spectrometry and scanning electron microscopy, Cell .Mol. Biol. 45 (1999) 793–803.
[17] M.D. Morris, S. Stewart, C.P. Tarnowski, D. Shea, R. Franceschi, D. Wang, M.A. Ignelzi Jr., W. Wang, E.T. Keller, D.L. Lin, S.A. Goldstein, J.M. Taboas, Early mineralization of normal and pathologic calvaria as revealed by Raman spectroscopy, SPIE Proc. 4614 (2002) 28–39.
[18] A. Carden, M.D. Morris, Application of vibrational spectroscopy to the study of mineralized tissues (review), J. Biomed. Opt. 5 (2000) 259–268.
[19] J.A. Timlin, A. Carden, M.D. Morris, Chemical microstructure of cortical bone probeb by Raman transects, Appl. Spectrosc. 53 (1999) 1429–1435.
[20] G. Penel, C. Delfosse, M. Descamps, G. Leroy, Composition of boné and apatitic biomaterials as revealed by intravital Raman microspectroscopy, Bone 36 (2005) 893–901.
[21] E.K. Morrie, Red-yellow marrow conversion: its effect on the location of some solitary bone lesions, J. Skelet. Radiol. 14 (1985) 10–19.